AIP | Applied Physics Letters

Fabrication of stereo metallic resonant structures with polymer droplets as template

Xiao-Chun Chen, Yuan-Wei Wu, Yu-Hui Hu, Hong-Min Li, Ru-Wen Peng et al.

Citation: Appl. Phys. Lett. **102**, 021904 (2013); doi: 10.1063/1.4775765
View online: http://dx.doi.org/10.1063/1.4775765
View Table of Contents: http://apl.aip.org/resource/1/APPLAB/v102/i2
Published by the American Institute of Physics.

Fabrication of stereo metallic resonant structures with polymer droplets as template

Xiao-Chun Chen, Yuan-Wei Wu, Yu-Hui Hu, Hong-Min Li, Ru-Wen Peng, Xi-Ping Hao, and Mu Wang[a)]
National Laboratory of Solid State Microstructures and Department of Physics, Nanjing University, Nanjing 210093, China

(Received 29 September 2012; accepted 27 December 2012; published online 15 January 2013)

Using polymer droplets formed in dewetting of polymer film on silicon surface as template, the silicon columns capped with circular polymer plates are fabricated via plasma etching. By blanket deposition of a gold layer on the structure, an array of metallic microcavities featured by a metal circular plate separated by a silicon column with the bottom metallic film is achieved. The geometrical parameters of the stereo structures can be tuned. We show that the electric field at the edge of the cap is greatly enhanced, which can be used as the hot spot for trace amount of chemical detection. © *2013 American Institute of Physics*. [http://dx.doi.org/10.1063/1.4775765]

Surface plasmon polariton (SPP) is the collective oscillation of free electrons on the metal–dielectric interface driven by the incident electromagnetic waves. If the momentum of the incident electromagnetic wave matches that of SPP, the incident wave may excite SPPs on the metal–dielectric interface.[1,2] In this process, alien molecules adsorbed on the metal surface will sensitively influence the resonance of the surface plasmon.[3] In many detection methods, various kinds of cavity structures are usually designed.[4–7] For the dielectric resonators, Q factor is extremely high. Yet for the plasmonic cavity, Q factor has been limited to just a few tens,[8,9] which is mainly due to the electromagnetic loss of metal material. Despite the strong loss of the metallic structure, however, the local SPP resonance (usually termed as "hot spots") on metallic structure remains very strong, which makes it possible to apply these structures as sensing devices.[10,11]

It is worthwhile to mention that the surface enhanced Raman scattering (SERS), initially observed in 1974, has been widely applied in chemical and biological sensing.[10,11] Especially the nanogap between metal particles has been discovered to associate with huge local electromagnetic field enhancement,[12–14] which is the physical origin for surface-enhanced spectroscopy[3] and some other nonlinear effects.[15,16] Many structures have been developed so far for sensing purpose, such as metal nanoshell,[17] metal nanoparticles,[18–20] nanoporous gold films,[21] etc. Despite that these metallic structures provide very high field enhancement factor, their stability and reproducibility remain the major limiting factors in applications. For high reproducibility, nanofabrications with prestige facilities such as focused ion beam[22] or electron beam lithography[23] are usually applied, yet these approaches are usually time consuming and expensive. Moreover, defects can be introduced in the patterning process, which might act as scattering centers and decrease the detection efficiency.

We present here a unique approach to fabricate stereo structures of gold-capped silicon pillars with the aim to develop an inexpensive, efficient way to make SERS substrate. We show that the geometrical parameters of the stereo metallic structure can be experimentally tuned. The edge of circular gold plate on top of the silicon column can act as the "hot spots" in detecting trace amount of absorption chemicals.

The polymer solution is prepared by dissolving a mixture of polystyrene (PS) (10 k, Mw = 9.58 kg/mol, Mw/Mn = 1.03, Fluka) and poly(methylmethacrylate) (PMMA) (10 k, Mw = 9.98 kg/mol, Mw/Mn = 1.03, Fluka) (1:1, W/W) in 99.5% pure toluene. The solution is then spin-coated on silicon substrate at 3000 rpm. The spin-coated thin film sample is annealed at 150 °C for 48 h so as to form circular polymer droplets on silicon surface. The silicon substrate with polymer droplets is then etched with SF_4 by inductively coupled plasma (ICP, ULVAC CE300i). Eventually an array of silicon pillars capped with a circular polymer plates is generated. Thereafter a gold film 30 nm in thickness is blanket deposited on the structure by electron beam evaporation. The optical properties are measured by microRaman spectroscopy (Renishaw) for SERS with Rhodamine 6G (R6G, Fluka) as the probing molecules. To carry out SERS measurements, the sample is immersed in 1.0 μM aqueous solution of R6G, douched with ethanol, and then dried in nitrogen gas. Cathodoluminescent spectroscopy (Gatan MonoCL4) is also used to investigate the excitation of surface plasmon on the structured surface.

The morphologies of the spin-coated PMMA/PS polymer blend film on silicon substrate before and after annealing are shown in Figs. 1(a) and 1(b), respectively. The circular bumps in Fig. 1(b) are the polymer droplets. As demonstrated in Refs. 24–26, each droplet possesses a PS kernel surrounded by a rim of PMMA. The ICP-etched structure is illustrated in Fig. 1(c). By tuning the strength and duration of etching, an ultrathin polymer plate is generated on top of the silicon column, and a cavity structure is generated.

The etched structure is then blanket deposited with gold, as shown in Fig. 2(a). The cross-section of the sample is shown in Fig. 2(b), from which the height of the structure can be accurately measured. It is clear that the capping on

a)Author to whom correspondence should be addressed. E-mail: muwang@nju.edu.cn.

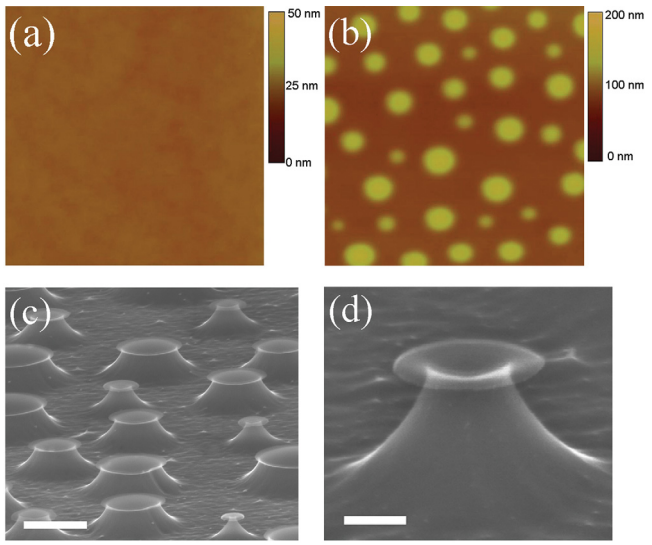

FIG. 1. AFM micrographs of the spin-coated PS/PMMA blend film before anneal (a) and after anneal (b). (c) and (d) represent the SEM micrograph of the cavities created by ICP etching with polymer droplets as template. The scan size is 10 μm for (a) and (b). The scale bar represents 1 μm in (c) and 200 nm in (d), respectively.

the top of the silicon column has played the role of shelter in blanket deposition of gold and lead to the gap of metal film on the side wall of the silicon column, as shown in Fig. 2(b). This discontinuity of the metal film is essential in SERS measurements. The size of the metallic cap on the top of the silicon column has been measured, and the histogram of the diameter distribution is shown in Fig. 2(c). The most probable diameter (D_p) locates at about 1.3 μm for the experimental conditions we selected and can be tuned by changing the initial thickness of the polymer film (Fig. 2(d)) and the time for plasma etching as well.

The optical properties of the stereo metallic structure (with D_p around 1.3 μm) has been numerically simulated by full-wave analysis (the green line in Fig. 3) and experimentally measured by a vacuum infrared Fourier transform

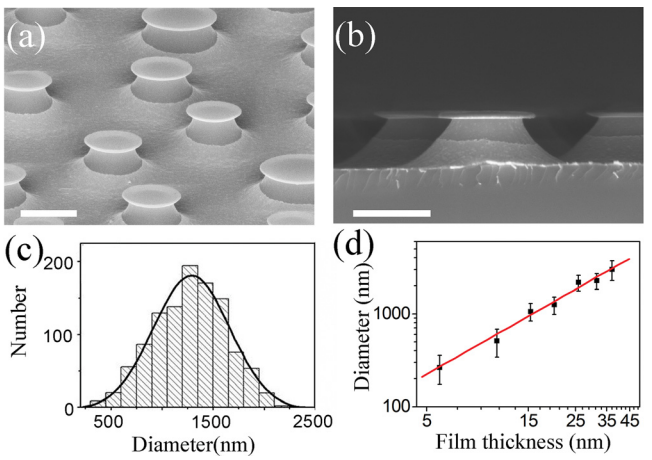

FIG. 2. (a) SEM micrograph of microcavities with gold capping on top of silicon columns. Substrate is also covered with a gold layer. (b) SEM micrograph of the micro cavity viewed from the side. (c) Histogram of the size of metallic capping on top of the silicon column. (d) Most probable diameter of the cap determined from the statistic graphs as that shown in (c) at different initial thickness of the PS/PMMA blend film. The scale bars in (a) and (b) represent 1 μm.

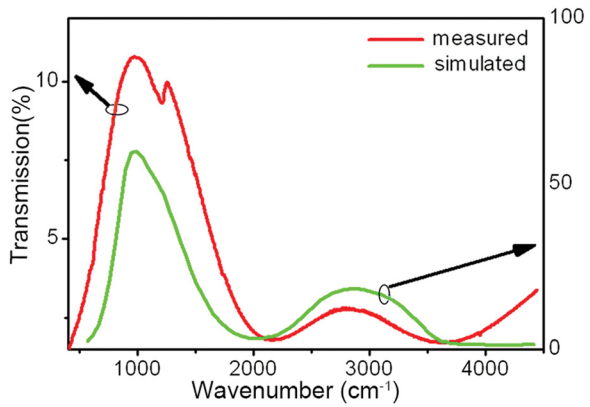

FIG. 3. The measured and simulated transmission spectra of microcavities with $D_p = 1300$ nm.

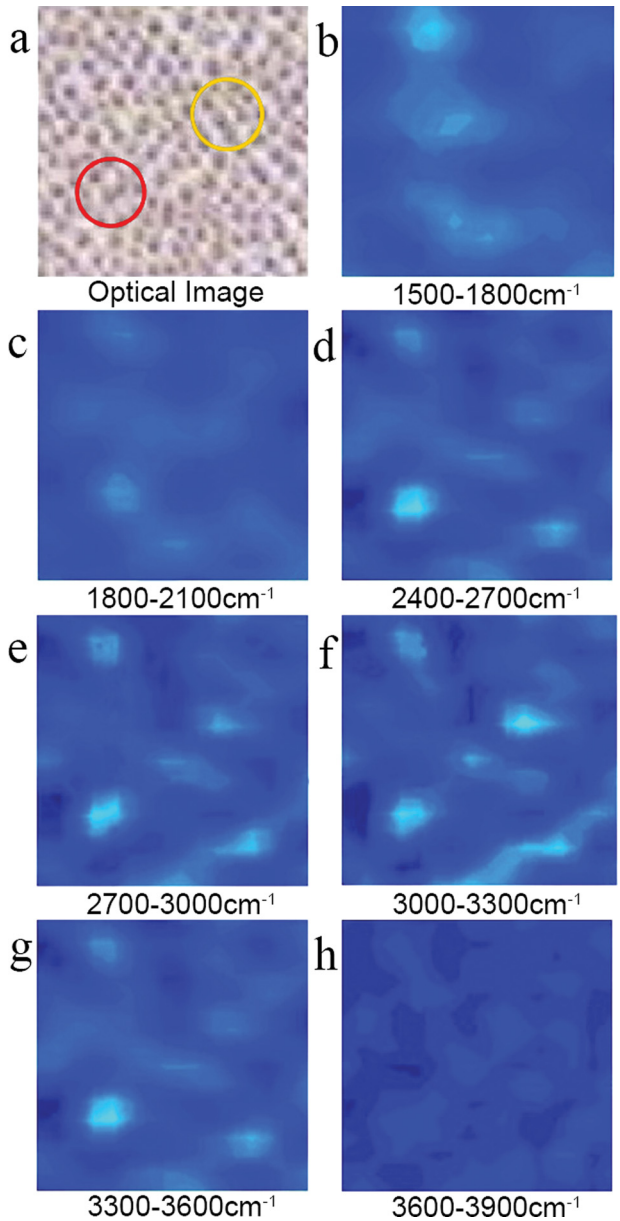

FIG. 4. FPA spectroscopy studies on the array of micro cavities with $D_p = 750$ nm. (a) Optical microscopy of the micro cavities. (b)–(h) show the integration over the wave numbers indicated below each frame. The structures within the yellow circle are excited in 3000 cm^{-1}–3300 cm^{-1}, those inside the red circle are excited in 2400 cm^{-1}–3600 cm^{-1}.

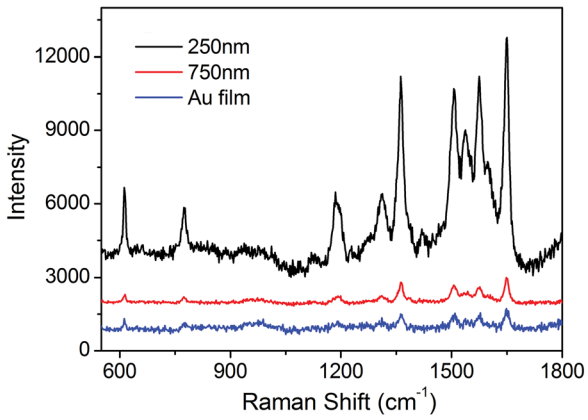

FIG. 5. SERS spectra of R6G measured on different substrates. The black line is measured from the substrate with micro cavities $D_p = 250$ nm. For the red line $D_p = 750$ nm. The blue line is measured from a flat Au film.

spectrometer (Bruker Vertex 70v) (the red line in Fig. 3). Two distinct extraordinary optical transmission (EOT) peaks can be identified, which are expected to associate with the localized surface plasmon resonance. To confirm this analysis, the metallic structures with $D_p = 750$ nm are measured by focal plane array (FPA) spectroscopy associated with Fourier transform infrared spectrometer. Figure 4(a) illustrates the optical micrograph of the structure; Figs. 4(b)–4(h) show the response of the same area at different range of wave numbers. We inspect, respectively, two areas marked by the red and yellow circles in Fig. 4(a). The droplets within the red circle are excited in the range 2400 cm^{-1}–3300 cm^{-1}, whereas those within yellow circle are excited in the range 3000 cm^{-1}–3300 cm^{-1}. Figure 4 shows that the excitation of metallic cavities depends on their geometrical parameters, and within the yellow circle the size distribution of the structure should be narrower than that within the red circle.

SERS spectra of R6G measured from different surfaces are illustrated in Fig. 5, where the black and red lines represent the SERS spectra from the metallic cavity structures with $D_p = 250$ nm and $D_p = 750$ nm, respectively. The blue line is measured from a flat gold film without any structure. All the spectra are collected with the same experimental conditions. The SERS signal of R6G from the cavity structure with $D_p = 250$ nm is significantly enhanced comparing with the other two spectra, which is expected to be the result of the field enhancement along the edge of the metallic cap on the top of silicon column.

The distribution of electric field around the metallic stereo structures with different geometrical parameters has been calculated with finite difference time domain (FDTD) method. Monochromic plane wave (514 nm) shines on the metal-capped structure with normal incidence to the capping plate. For the microcavity with diameter 250 nm (Figs. 6(a) and 4(b)), the enhancement factor of localized electric field is around 20. For the microcavity with diameter 750 nm, however, no obvious enhancement can be detected (Figs. 6(c) and 6(d)).

The selective enhancement of the electric field on the edge of the caps is directly observed with cathodoluminescence (CL) spectroscopy. Excited by the electron beams, SPP can be generated on metal surface.[27,28] However,

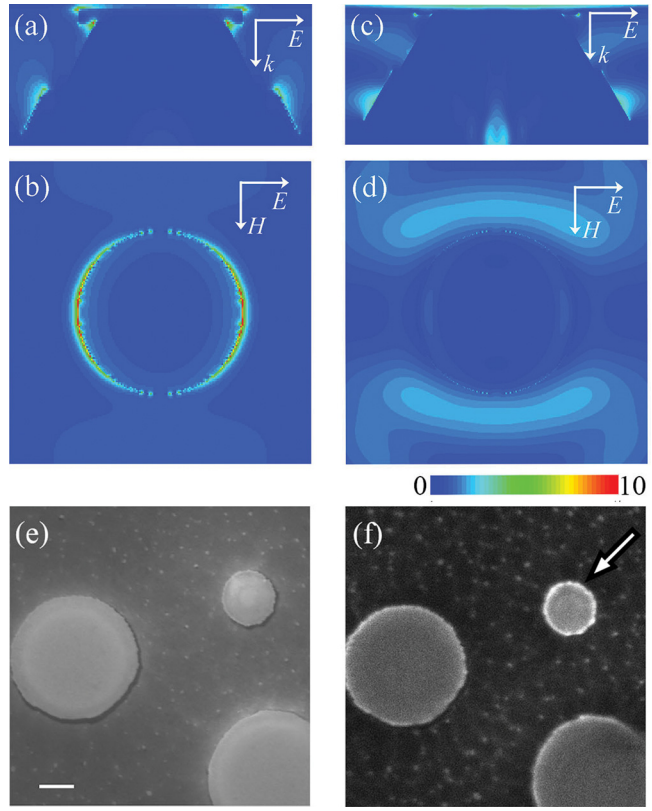

FIG. 6. Simulated electrical field ($|E|/|E_0|$) on a single cavity with excitation wave length as 514 nm ((a)–(d)) and the CL spectroscopy on the metallic cavities ((e)–(f)). (a) and (b) show the side and top view of the field distribution with cap size 250 nm. (c) and (d) show the situation when the cap size is changed to 750 nm. (e) shows the top-view SEM micrograph of the cavities. (f) is the corresponding CL imaging with whole wavelength light collection. The smaller disk has a brightened rim. The scale bar represents 500 nm.

whether the resonance can be induced depends on the geometrical parameters of the cavities. Figure 6(e) illustrates the SEM micrograph viewed from the top, and Fig. 6(f) shows the CL micrograph of the structure. The smaller structure has been lightened evidently on the edge (as marked by the white arrow), whereas the larger cavities remain dim on the edges. The experimental data confirm the simulated results.

In our experiments, we consider the electromagnetic enhancement as the major contributor to SERS. As the first order approximation, its contribution is proportional to the fourth power of the field enhancement. We therefore estimate that at the edge of the circular plate, the electromagnetic enhancement factor can reach 5×10^4 based on the data in Figs. 6(a)–6(d).

Detecting trace amount of chemicals with low cost and high reliability is an important task nowadays. In this letter we demonstrate a very simple way to fabricate metallic microcavities. Each cavity can be considered as a gold-capped silicon pillar standing on a gold film. The average size of the cavities can be tuned by changing the initial thickness of polymer blend film, and the ratio of cap size and column height depends on the duration and strength of etching. SERS spectra indicate that micro cavities with $D_p = 250$ nm may work as a good SERS substrate for molecular detection with 514 nm laser incidence. The electromagnetic enhancement at the edge of the cavity has been calculated and directly observed with cathodoluminescence. We suggest

that the system we report here provides an easy approach for trace amount of alien molecule detection.

This work has been supported by the grants from the MOST of China (Grant Nos. 2010CB630705 and 2012CB921502), the NSF of China (Grant Nos. 50972057, 11034005, and 61077023), and partly by Jiangsu Province (Grant No. BK2008012).

[1]A. V. Zayats, I. I. Smolyaninov, and A. A. Maradudin, Phys. Rep. **408**, 131 (2005).
[2]H. R. Raether, *Surface Plasmons on Smooth and Rough Surfaces and on Gratings* (Springer, 1988).
[3]M. Moskovits, Rev. Mod. Phys. **57**, 783 (1985).
[4]B. Min, E. Ostby, V. Sorger, E. Ulin-Avila, L. Yang, X. Zhang, and K. Vahala, Nature **457**, 455 (2009).
[5]Q. Min and R. Gordon, Opt. Express **16**, 9708 (2008).
[6]C. Y. Ding, X. Y. Hu, P. Jiang, and Q. H. Gong, Phys. Lett. A **372**, 4536 (2008).
[7]M. W. Tsai, T. H. Chuang, C. Y. Meng, Y. T. Chang, and S. C. Lee, Appl. Phys. Lett. **89**, 173116 (2006).
[8]E. J. R. Vesseur, R. de Waele, H. J. Lezec, H. A. Atwater, F. J. García de Abajo, and A. Polman, Appl. Phys. Lett. **92**, 083110 (2008).
[9]Y. H. Chen and L. J. Guo, Plasmonics **6**, 183 (2011).
[10]K. A. Willets and R. P. Van Duyne, Annu. Rev. Phys. Chem. **58**, 267 (2007).
[11]P. L. Stiles, J. A. Dieringer, N. C. Shah, and R. P. Van Duyne, Annu. Rev. Anal. Chem. **1**, 601 (2008).
[12]T. Atay, J. H. Song, and A. V. Nurmikko, Nano Lett. **4**, 1627 (2004).
[13]H. X. Xu, E. J. Bjerneld, M. Kall, and L. Borjesson, Phys. Rev. Lett. **83**, 4357 (1999).
[14]H. X. Xu, J. Aizpurua, M. Kall, and P. Apell, Phys. Rev. E **62**, 4318 (2000).
[15]A. Campion and P. Kambhampati, Chem. Soc. Rev. **27**, 241 (1998).
[16]I. V. Baca, A. P. Brown, M. P. Andrews, T. Galstian, Y. Li, H. Vali, and M. G. Kuzyk, Can. J. Chem. **80**, 1625 (2002).
[17]L. R. Hirsch, A. M. Gobin, A. R. Lowery, F. Tam, R. A. Drezek, N. J. Halas, and J. L. West, Ann. Biomed. Eng. **34**, 15 (2006).
[18]B. B. Huang, J. Y. Wang, S. J. Huo, and W. B. Cai, Surf. Interface Anal. **40**, 81 (2008).
[19]K. L. Kelly, E. Coronado, L. L. Zhao, and G. C. Schatz, J. Phys. Chem. B **107**, 668 (2003).
[20]C. J. Murphy, T. K. Sau, A. M. Gole, C. J. G. Orendorff, J. L. Gou, S. E. Hunyadi, and T. Li, J. Phys. Chem. B **109**, 13857 (2005).
[21]A. I. Maaroof, A. Gentle, G. B. Smith, and M. B. Cortie, J. Phys. D: Appl. Phys. **40**, 5675 (2007).
[22]J. Aizpurua, P. Hanarp, D. S. Sutherland, M. Käll, G. W. Bryanta, and F. J. García de Abajob, Phys. Rev. Lett. **90**, 057401 (2003)
[23]M. Kahl, E. Voges, S. Kostrewa, C. Viets, and W. Hill, Sens. Actuators B **51**, 285 (1998).
[24]M. Harris, G. Appel, and H. Ade, Macromolecules **36**, 3307–3314 (2003).
[25]Y. Li, Y. Yang, F. Yu, and L. S. Dong, J. Polym. Sci., Part B: Polym. Phys. **44**, 9–21 (2006).
[26]X. C. Chen, H. M. Li, F. Fang, Y. W. Wu, M. Wang, G. B. Ma, Y. Q. Ma, D. J. Shu, and R. W. Peng, Adv. Mater. **24**, 2637–2641 (2012).
[27]C. E. Hofmann, E. J. R. Vesseur, L. A. Sweatlock, H. J. Lezec, F. J. García de Abajo, A. Polman, and H. A. Atwater, Nano Lett. **7**, 3612 (2007).
[28]X. L. Zhu, J. S. Zhang, J. Xu, and D. P. Yu, Nano Lett. **11**, 1117 (2011).